A process model for active brazing of ceramics

Part II *Optimization of brazing conditions and joint properties*

T. TORVUND, Ø. GRONG
Department of Metallurgy, Norwegian University of Science and Technology, N-7034 Trondheim, Norway

O. M. AKSELSEN, J. H. ULVENSØEN
SINTEF – Materials Technology, N-7034 Trondheim, Norway

In the present investigation, the process model developed in Part I has been applied to evaluate the microstructure and strength evolution during active brazing of ceramics. As a starting point, reaction-layer growth is assumed to occur isothermally with no restrictions in the supply of reactive element. Different kinds of diagrams are then constructed to show how specific process variables (e.g. the heating and cooling period, the limiting layer thickness, and the diffusion mechanism) affect the growth kinetics. It is concluded that the key to improved joint properties lies in control of the reaction-layer thickness through optimization of the brazing conditions, and an illustration of this is given.

Nomenclature

C	Concentration of active element in braze alloy
CR	Cooling rate ($^\circ$C s^{-1})
FDCA	Finite diffusion couple analogue
HR	Heating rate ($^\circ$C s^{-1})
IDCA	Infinite diffusion couple analogue
k_0^*	Rate constant referring to infinite diffusion couple analogue (m^2 s^{-1})
k_p	Parabolic growth rate constant (m^2 s^{-1})
L	Half-width of braze metal zone (m)
PGL	Parabolic growth law
Q_{app}^*	Apparent activation energy for diffusion (J mol^{-1})
R	Universal gas constant
t	Time (s)
t_0	Incubation time (s)
t_1, t_2	Limits of integration (s)
t_i	Isothermal hold time (s)
T	Absolute temperature (K or $^\circ$C)
T_c	Chosen reference temperature (K or $^\circ$C)
T_i	Isothermal hold temperature (K or $^\circ$C)
X	Thickness of reaction layer (m)
X_{lim}	Limiting thickness of reaction layer (m)
σ_f	Shear strength (MPa)

1. Introduction

The interest in process modelling has gained considerable momentum over the past decade [1, 2]. The major impetus for this development has been provided by the needs of industry to improve productivity and product quality. However, process models are also valuable from an academic point of view, because they provide the user with basic knowledge of the behaviour of materials during processing and can serve as a means to consolidate scientific knowledge about a specific process or class of material.

Process modelling is currently seen as a strategic commercial issue by the manufacturing industry to reach the goal of faster process development and optimization of joint properties [1, 2]. A metallurgical process model draws together established knowledge of the kinetics of microstructure evolution with dislocation or fracture behaviour in order to determine the resulting mechanical properties [3–5]. An important feature of the method is to maintain a consistent level of accuracy in all of the components of the model. It is also desirable to keep the models as simple as possible to make them quick and easy to implement and accessible to potential industry users. These two considerations suggest the use of approximative, analytical solutions within the scope of personal computers [5].

The process model developed in Part I of this investigation [6] combines information about the thermodynamics of different ceramic–metal systems with kinetic data to describe reaction-layer growth during active brazing of ceramics. Here, the microstructure evolution is captured mathematically in terms of differential variation of the primary state variable with time. The differential equation is then integrated through the thermal history to allow for transient effects during heating and cooling as well as changes in the growth kinetics due to restrictions in the supply of the active component. In the present

paper, the aptness and limitations of this approach are further elaborated and explored. As a starting point, the process model will be applied to the materials considered in Part I [6]. Subsequently, its potentials for braze metal alloy design and optimization of brazing cycles for specific ceramic-ceramic combinations will be illustrated in different numerical examples and case studies.

2. Interrogation of the process model
In general, reaction-layer growth during active brazing of ceramics depends on the interplay between a number of variables which cannot readily be accounted for in a simple mathematical simulation of the process. Referring to Fig. 1, the process parameters allowed for in the present model are the heating leg of the brazing cycle, the isothermal hold period, the cooling period, and the initial content (mass) of reactive element in the braze metal. By considering the stoichiometry of the displacement reaction at the ceramic/braze metal interface and the diffusion mechanism involved, the reaction layer thickness can be calculated as a function of time and temperature for fixed starting conditions. The results may then be plotted on different kinds of brazing diagrams to display the growth kinetics. In this section, a three-dimensional graphical representation has been chosen to illustrate how specific process parameters and kinetic variables affect the microstructure evolution. Here the image of the layer thickness is captured in the form of a curved surface in temperature–time space.

2.1. Materials combinations
As a starting point, we consider brazing of Si_3N_4 with Cu–Ti based filler metals. The Si_3N_4/Cu–Ti system can be classified as an infinite diffusion couple analogue (IDCA) according to the definition in Part I [6], but in the context of this study, the assumption will be relaxed in order to illustrate reaction-layer growth under different operating conditions. A summary of input data is given in Table I.

2.2. Isothermal growth of reaction layers
In its simplest form, the parabolic growth law describes the evolution of the reaction layer as a function of time and temperature for an infinite diffusion couple. In the present context this essentially means that there is no restriction in the supply of the active element during brazing which may lead to a change in the growth kinetics. Fig. 2 shows a three-dimensional
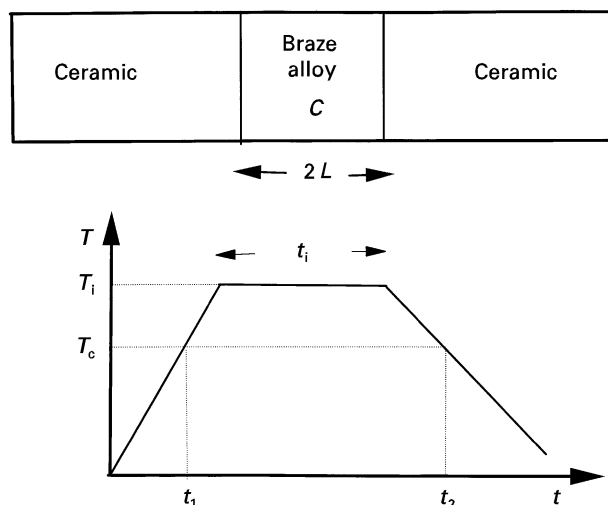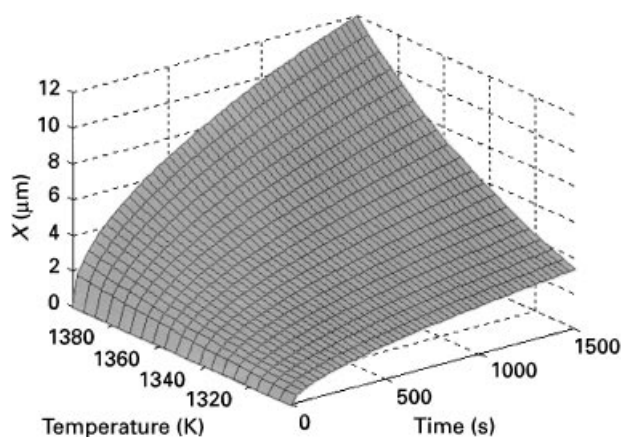

Figure 1 Sketch of the model system.

Figure 2 Graphical representation of the reaction-layer thickness, as predicted from the parabolic growth law.

graphical representation of the layer thickness under such conditions.

However, in a real brazing situation due consideration must also be given to the amount of active element consumed in reactions with the ceramic. This, in turn, requires information about the phase relations at the ceramic/braze metal interface in the form of a stoichiometrically balanced displacement reaction [6]. As an illustration of principles, we shall assume that the total mass of active element initially present in the braze metal corresponds to a limiting layer thickness, X_{lim}, of 6 µm, as indicated in Table 1. The system may respond to this restriction in two different ways. If the response is similar to that of the infinite diffusion couple analogue (see Fig. 3a), growth will proceed

TABLE I Input data used in modelling exercises: from [6, 8]

System	Heat. rate (°C s^{-1})	Cool. rate (°C s^{-1})	k_0^* (µm^2 s^{-1})	Q_{app}^* (kJ mol^{-1})	X_{lim} (µm)	T_c (°C)
Si_3N_4/Cu–Ti	0.5	0.5	1.3×10^{14}	405	6[a]	1030
Al_2O_3/Ag–Cu–Ti	0.25	0.08	1.0×10^6	190	> 26[b]	800

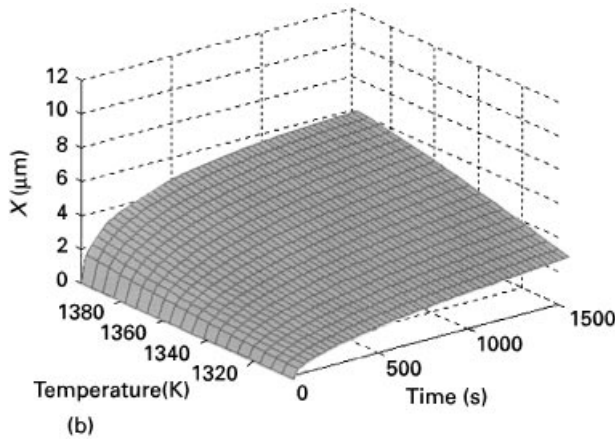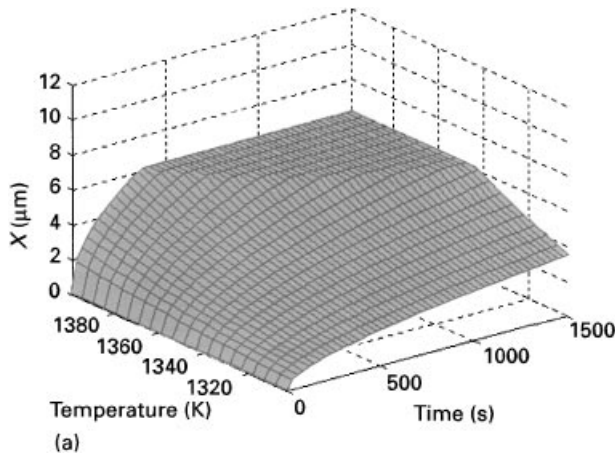[a] $2L = 0.1$ mm.
[b] $2L = 0.7$ mm.

4438

Figure 3 Predicted change in the reaction-layer growth kinetics due to restriction in supply of the reactive element; (a) infinite diffusion couple analogue, (b) finite diffusion couple analogue.

Figure 4 Graphical representation of the reaction-layer thickness after inclusion of the transient heating and cooling period; (a) infinite diffusion couple analogue, (b) finite diffusion couple analogue.

unhindered by the element consumption until the process suddenly stops at $X = X_{lim}$ when all active element is tied up in the reaction product. In contrast, the assumption of a finite diffusion couple analogue (FDCA) implies that the growth process is gradually slowed down as the reaction proceeds and hence, X_{lim} is approached in an asymptotic rather than an abrupt manner, as illustrated in Fig. 3b. Both growth modes have been observed during active brazing of ceramics, and reflect a difference in the diffusion mechanism [6].

2.3. Non-isothermal growth of reaction layers

Because active brazing is normally carried out in a vacuum furnace with a limited heating and cooling capacity, extensive reaction-layer growth may occur during the transient part of the brazing cycle. Methods have been outlined in Part I of this investigation [6] for handling the non-isothermal case by means of process modelling techniques. In the following, this important aspect of the brazing process is further elaborated and explored.

Fig. 4a shows a three-dimensional graphical representation of the layer thickness for the same starting conditions as in Fig. 2, with the exception that a correction n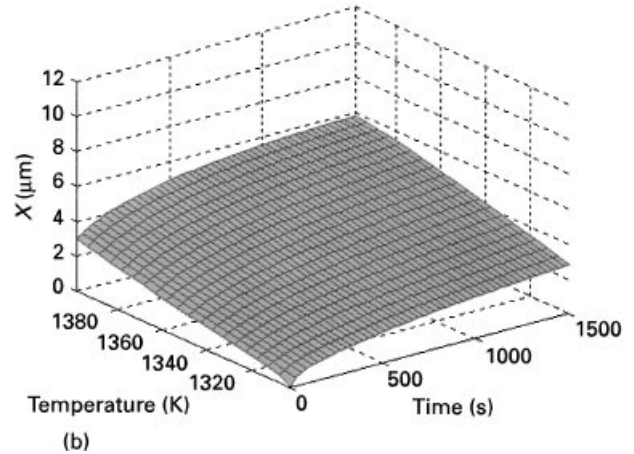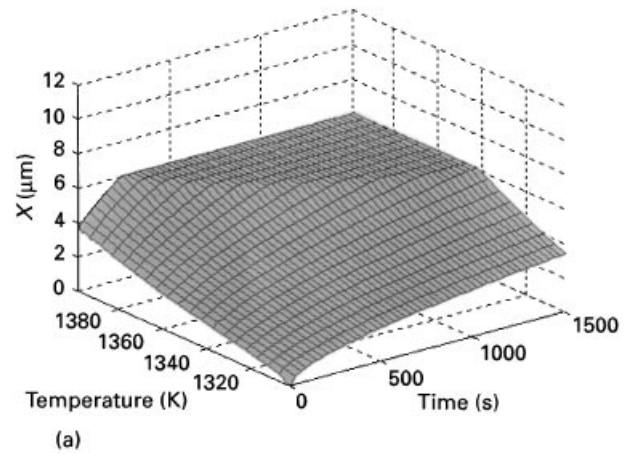ow is included for the contribution of the heating and cooling leg of the thermal cycle to the total layer thickness (indicated by the vertical section at $t = 0$ in the diagrams). It follows that the extent to which the transient heating and cooling period contributes to reaction-layer growth depends on the operational conditions applied. Generally, the use of a low heating and cooling rate in combination with a high brazing temperature implies that the transient growth period will completely dominate the evolution process, as shown in Fig. 4a. In practice, this is seen as a large deviation from the parabolic growth law. The contribution is less apparent during rapid heating and cooling (not shown here), but transient effects may still influence the growth kinetics if the isothermal hold period is sufficiently short compared with the total time spent in the thermal cycle. Owing to the assumption of abundant supply of reactive element, both the heating and the cooling period will contribute equally to reaction-layer growth under the prevailing circumstances, provided that the kinetic strength of the thermal cycles is the same. This means that the thermal path is not implicitly built into the model.

The situation is different if the diffusion is restricted by supply of the active component in the braze metal. Under such conditions there is no simple relation between growth which occurs during the various steps of the brazing process because the reaction is

4439

thermal path dependent. Hence, the contribution from the heating leg of the thermal cycle will normally be more important than the contributions from the isothermal hold period and the cooling leg of the thermal cycle, leading to an overall reduction in the total layer thickness, as shown in Fig. 4b. Integration of the differential evolution equation must then be carried out stepwise in time over the predetermined thermal cycle, using the solution method described in Part I [6].

2.4. Deviations from the parabolic growth law

The parabolic growth law (PGL) is based on the assumption that the same diffusion mechanism is operating during the whole evolution process. When the heating and cooling legs of the thermal cycle are neglected, this essentially means that a plot of the layer thickness versus the square root of the brazing time should yield a straight line passing through the origin, according to the relationship

$$X = (k_p t)^{1/2} \qquad (1)$$

where k_p is the parabolic growth rate constant.

Normally, a deviation from the expected relationship is interpreted as a change in diffusion mechanism, but in the case of active brazing of ceramics the picture is generally more complex because of the number of side reactions involved. In the following, attempts will be made to rationalize the individual and combined contributions of some of these side reactions in terms of the process model developed in Part I [6].

Fig. 5a shows plots of typical X–$t^{1/2}$ curves under isothermal heat-treatment conditions for the three model systems considered above. As expected, the infinite diffusion couple analogue is well represented by the parabolic growth law up to $X = X_{lim}$, where the growth process suddenly stops when all the active element is consumed in reactions with the ceramic. The lines representing PGL and X_{lim} in the diagram will, in turn, be asymptotes for the finite diffusion couple analogue, which are approached in the limit when $X \ll X_{lim}$ and $t_i \rightarrow \infty$, respectively. The deviation from the parabolic growth law becomes even more striking if a correction also is included for the amount of growth which occurs during heating and cooling. In the latter case, the PGL line has no direct physical meaning in the sense that it defines a meaningful asymptote in the diagram, as illustrated in Fig. 5b.

The plots in Fig. 5 are based on the assumption that the reaction takes place in the absence of a contaminating oxide film at the ceramic–metal interface, i.e. there is no initial barrier against diffusion. In the case of active brazing of ceramics this is not necessarily a good assumption, because the use of different joint preparation techniques may lead to extensive oxide skin formation. The normal way of handling the oxide contamination problem is to introduce an empirical incubation time, t_0, in the expression for the parabolic growth law to allow for sluggish layer growth during the early stages of the process [7]. In its simplest form,
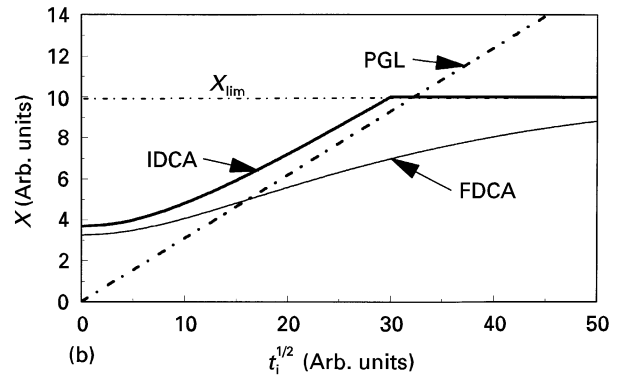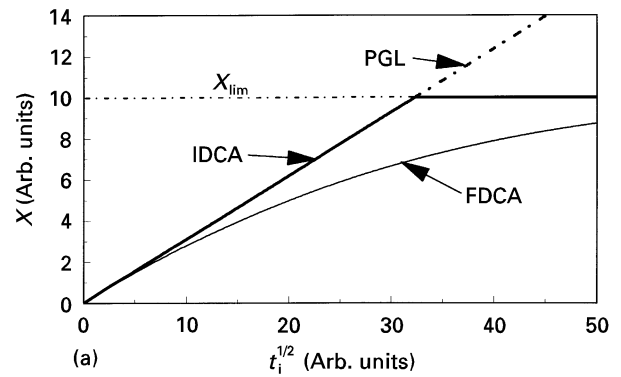

(a)

(b)

Figure 5 Plots of typical X–$t^{1/2}$ curves for different starting conditions; (a) isothermal growth of reaction layers, (b) non-isothermal growth of reaction layers.

the modified growth law can be written as:

$$X = [k_p(t - t_0)]^{1/2} \qquad (2)$$

The effect of t_0 on the growth kinetics under isothermal conditions can readily be inferred from the above relationship, i.e. the incubation time will have a strong influence on the X–$t^{1/2}$ curve during the early stages of the process, but is negligible after long holding times. In a real brazing situation, the picture is more complex, as shown in Fig. 6a and b, due to the combined action of the different side reactions involved. In both cases the presence of a contaminating oxide layer at the ceramic/metal interface will reduce the contribution from the transient heating period and lead to X–$t^{1/2}$ pattern that erroneously may be confused with parabolic growth. This, in turn, may give rise to misconceptions about the reaction mechanisms involved.

3. Optimization of joint properties
Brazed ceramic–ceramic joints are prime examples of components where the properties achieved depend upon the characteristics of the microstructure. Because the contribution from thermal contraction stresses in this case is small compared with ceramic–metal joints, a direct relationship exists between the joint shear strength, σ_f, and the reaction-layer thickness, X, as illustrated in Fig. 7. The inverted V-shaped curve in Fig. 7 reflects the fact that both the interfacial sliding resistance and the inclination to crack formation tend to increase with increasing values of X, which means that the highest shear strength is attained at an
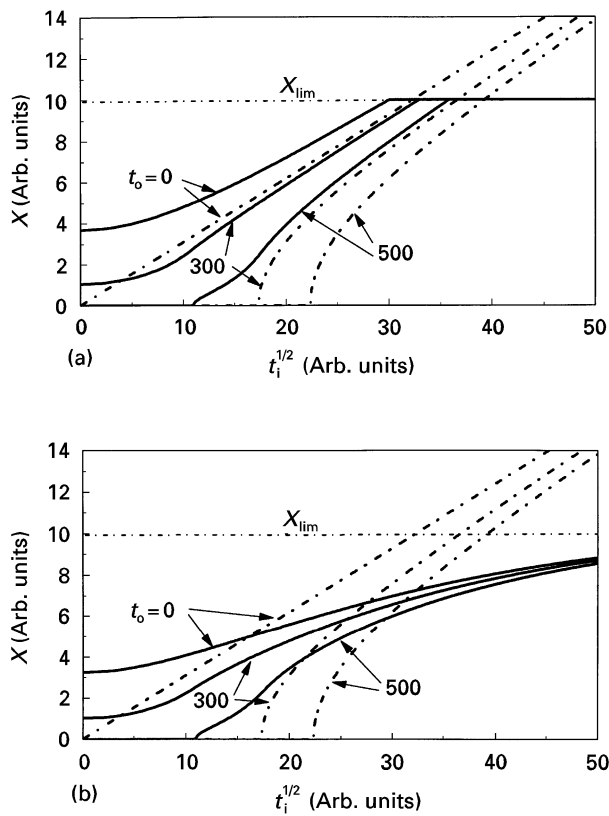
(a)

(b)

Figure 6 Predicted change in the shape of the X–$t^{1/2}$ curves after inclusion of the incubation time; (a) solid line: IDCA, (b) solid line: FDCA. Broken line: PGL.
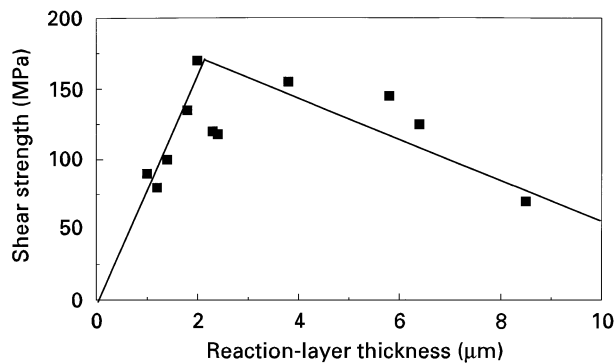

Figure 7 The relationship between joint shear strength and the reaction-layer thickness. The experimental data refer to brazing of Al_2O_3 with Ag-Cu-Ti filler metals. After Hongqi *et al.* [8].

3.1. Brazing of Al_2O_3 with Ag–Cu–Ti filler metals

The results in Fig. 7 refer to brazing of Al_2O_3 with Ag–Cu–Ti filler metals. Although different types of reaction products form at high and low brazing temperatures [8], the gross microstructure evolution may be described by a single set of parameters for the parabolic growth rate constant in the expression for
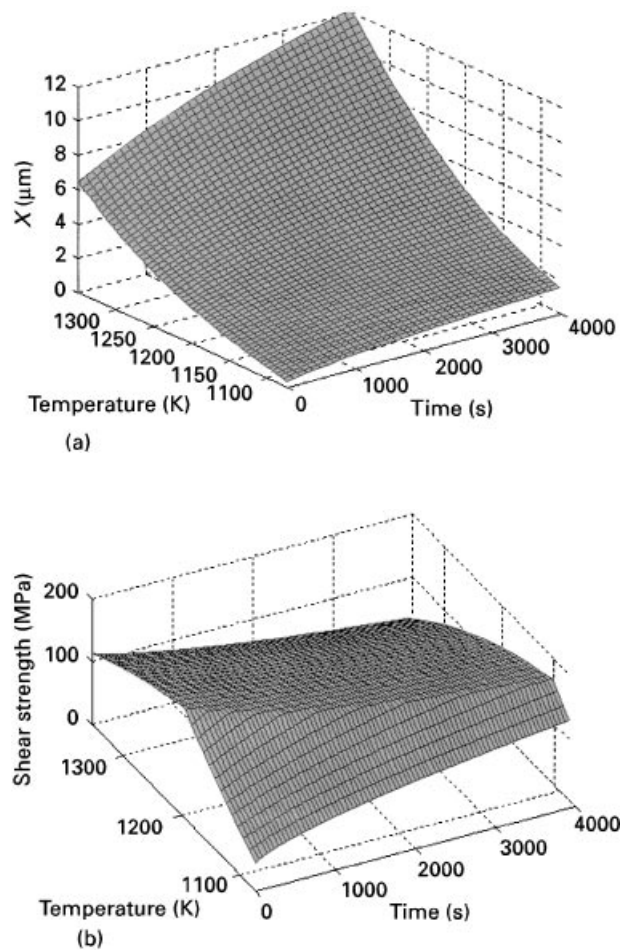

(a)

(b)

Figure 8 Predicted microstructure and strength evolution during brazing of Al_2O_3 with Ag–Cu–Ti filler metals; (a) reaction layer thickness, (b) resulting shear strength distribution. Operational conditions as in Table 1.

the finite diffusion couple analogue. Fig. 8a shows a three-dimensional graphical representation of the reaction-layer thickness, using input data from Table I. The resulting shear strength distribution is shown in Fig. 8b.

As expected, the contour representing the peak shear strength in Fig. 8b closely follows the contour defining the 2 μm reaction layer thickness in Fig. 8a. In a real brazing situation, this essentially means that the shear strength will pass through a local maximum if σ_f is plotted against either the brazing temperature or the isothermal hold time for fixed starting conditions. This type of response is well documented in the scientific literature [8–13].

3.2. Process diagrams

By utilizing the process model developed in Part I [6], it is also possible to predict behaviour under conditions which have not yet been studied. Examples of such computations are shown in Fig. 9. It is evident from these diagrams that the locus of the peak strength in temperature–time space depends strongly on the operating conditions applied (e.g. the heating and cooling rate or the total amount of active element present in the filler metal). Because the former parameters are usually not recorded during brazing, the
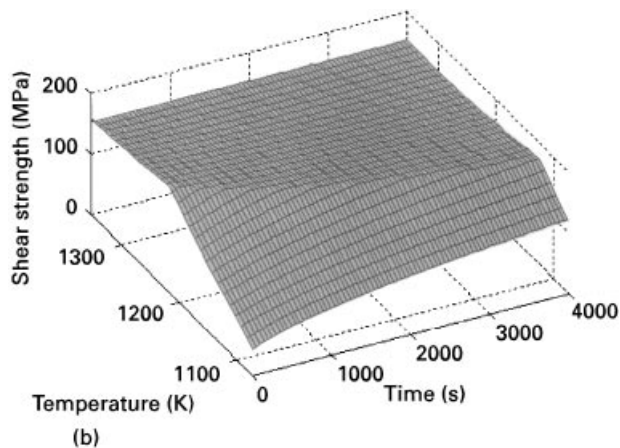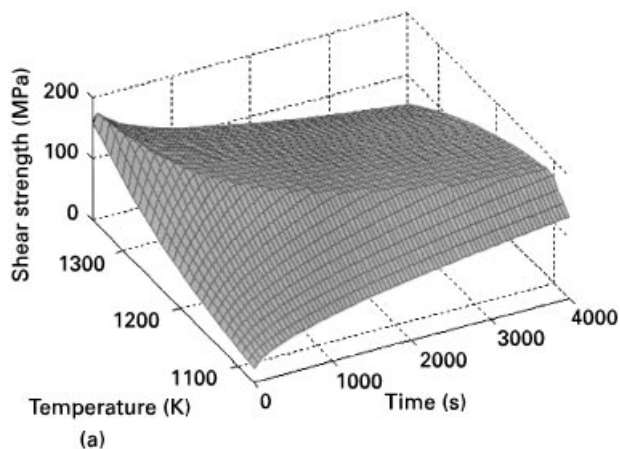
intermediate layer thickness (here about 2 μm) [8]. This shows that there is a great potential for optimization of joint properties through control of the filler metal composition and the temperature–time pattern during brazing.

4441

Figure 9 Brazing diagrams for Al_2O_3/Ag–Cu–Ti joints; (a) effect of heating and cooling rate on joint shear strength (HR = CR = $2\,°C\,s^{-1}$); (b) effect of width of braze metal zone on joint shear strength ($2L = 0.1$mm). Operational conditions as in Table 1 (with proper adjustments of input parameters).

properties achieved can deviate considerably from the expected values if the experiments are repeated in another environment. This represents a significant source of confusion, and makes a comparison with other literature data rather fortuitous.

4. Conclusion
In the present investigation process modelling techniques have been applied to evaluate the conditions for reaction layer growth during active brazing of ceramics. It is shown that the microstructure evolution depends on the interplay between a number of side reactions which cannot readily be accounted for in a simple analytical simulation of the process. In general, both the transient heating and cooling period as well as the total amount of active element present in the filler metal will influence the growth kinetics to an extent which makes predictions based on the parabolic growth law rather uncertain. This, in turn, may give rise to misconceptions about the reaction mechanisms involved.

Because a direct relationship exists between the shear strength, σ_f, and the reaction-layer thickness, there is a great potential for optimization of joint properties through control of the filler metal composition and the temperature–time pattern during brazing. Normally, the shear strength of ceramic–ceramic joints will pass through a local maximum if σ_f is plotted against either the brazing temperature or the isothermal hold time for fixed starting conditions. However, because the locus of the peak strength in temperature–time space depends on the operational conditions applied, the properties achieved are sensitive to variations in process variables, such as the heating and cooling rate and the total amount of active element present in the braze metal. The lack of adequate documentation of brazing parameters represents a significant source of confusion, and makes a comparison with other literature data rather fortuitous.

References
1. H. R. SHERCLIFF, P. SARGENT and B. WOOD, "Modelling Materials Processing" Cambridge University Engineering Department, Technical Report CUED/C-MATS/TR206 (1993).
2. M. F. ASHBY, *Mater. Sci. Technol.* **8** (1992) 102.
3. H. R. SHERCLIFF, O. R. MYHR and S. TJØTTA, *MRS Bull.* **XIX** (1994) 25.
4. H. R. SHERCLIFF, Ø. GRONG, O.R. MYHR and M.F. ASHBY, in "Proceedings of the 3rd International Conference on Aluminium Alloys", (ICAA3), Vol. III, Trondheim, June 1992, edited by L. Arnberg, O. Lohne, E. Nes and N. Ryum, (NTH-trykk, 1992) p. 357.
5. D. H. BRATLAND, Ø. GRONG, H. R. SHERCLIFF, O. R. MYHR and S. TJØTTA, *Acta Mater.*, **45** (1997) 1.
6. T. TORVUND, Ø. GRONG, O. M. AKSELSEN and J. H. ULVENSØEN *J. Mater. Sci.*, **31** (1996) 6215.
7. F. J. J. VAN LOO, *Prog. Solid St. Chem.* **20** (1990) 47.
8. H. HONGQI, J. ZHIHAO and W. XIAOTIAN, *J. Mater. Sci.* **29** (1994) 5041.
9. O. M. AKSELSEN, ibid. **27** (1992) 1989.
10. M. NAKA, T. TANAKA and I. OKAMOTO, *Trans. JWRI* **16** (1987) 83.
11. A. P. XIAN and Z. Y. SI, *J. Mater. Sci.* **25** (1990) 4483.
12. T. OKAMOTO, *ISIJ Int.* **30** (1990) 1033.
13. H. HONGQI, W. YONGLAN, J. ZHIHAO and W. XIAOTIAN, *J. Mater. Sci.* **30** (1995) 1233.